Product Distribution and Pre-Steady-State Kinetic Analysis of *Escherichia coli* Undecaprenyl Pyrophosphate Synthase Reaction†

Jian-Jung Pan, Shean-Tai Chiou, and Po-Huang Liang*

Institute of Biological Chemistry, Academia Sinica, Nankang, Taipei 11529, Taiwan

Received May 1, 2000

ABSTRACT: Undecaprenyl pyrophosphate synthase (UPPs) catalyzes the condensation of eight molecules of isopentenyl pyrophosphate (IPP) with farnesyl pyrophosphate (FPP) to generate C_{55} undecaprenyl pyrophosphate. We investigated the kinetics and mechanism of this reaction pathway using *Escherichia coli* UPPs. With a variety of different ratios of enzyme to substrate and FPP to IPP in the presence or absence of Triton, different product distributions were found. In the presence of excess FPP, the intermediates (C_{25}−C_{50}) accumulated. Under a condition with enzyme and FPP in excess of IPP, instead of C_{20}-geranylgeranyl pyrophosphate, C_{20}, C_{25}, and C_{30} were the major products. The UPPs steady-state k_{cat} value (2.5 s^{-1}) in the presence of 0.1% Triton was 190-fold larger than in the absence of Triton (0.013 s^{-1}). The k_{cat} value matched the rate constant of each IPP condensation obtained from the enzyme single-turnover experiments. This suggested that the IPP condensation rather than product release was the rate-limiting step in the presence of Triton. In the absence of Triton, the intermediates formed and disappeared in a similar manner under enzyme single turnover in contrast to the slow steady-state rate, which indicated a step after product generation was rate limiting. This was further supported by a burst product formation. Judging from the accumulation level of C_{55}, C_{60}, and C_{65}, their dissociation from the enzyme cannot be too slow and an even slower enzyme conformational change with a rate of 0.001 s^{-1} might govern the UPPs reaction rate under the steady-state condition in the absence of Triton.

In the biosynthesis of bacterial cell wall glycoconjugates, carbohydrates are made in the cytoplasma and covalently linked to the lipid carrier, C_{55}-undecaprenyl phosphate, for their transportation across the membrane (*1*). Undecaprenyl phosphate is generated from the dephosphorylation of undecaprenyl pyrophosphate (UPP)[1] which itself is the product of eight sequential condensations of isopentenyl pyrophosphate (IPP) with *trans,trans*-farnesyl pyrophosphate (*t*,*t*-FPP). This coupling reaction is catalyzed by the enzyme undecaprenyl pyrophosphate synthase (UPPs) as shown in Scheme 1 (*2*, *3*). UPPs enzymes have been partially purified and studied from *Lactobacillus plantarum*, *Micrococcus luteus*, and *Bacillus subtilis* bacteria (see ref *4* for a review). Recently, the gene encoding UPPs was identified from *M. luteus* (*5*) and later from 25 species including Gram (+) and Gram (−) bacteria (*6*). The enzyme was shown to be essential for growth of *Streptococcus pneumonia*e R6 (*6*).

UPPs is a member of prenyltransferase family but is unique from others in the product stereochemistry and chain length (*4*, *7*, *8*). Unlike many E-type enzymes which catalyze the syntheses of short and medium chain-length all-trans polyprenyl pyrophosphates, UPPs catalyzes long chain C_{55}-polyprenyl pyrophosphate synthesis with formed double bonds in cis configuration, and it is a Z-type enzyme. This long chain elongation enzyme was shown to require detergent or lipid for efficient enzyme turnover (*9*−*13*). This is probably due to the slow release of the hydrophobic product in the absence of Triton and/or Triton changes the enzyme conformation for activity. Triton can probably activate the UPPs by increasing the product dissociation rate that is rate limiting under steady-state condition. It is also possible that some other step such as a protein conformational change after

Scheme 1: Reaction Catalyzed by Undecaprenyl Pyrophosphate Synthase[a]

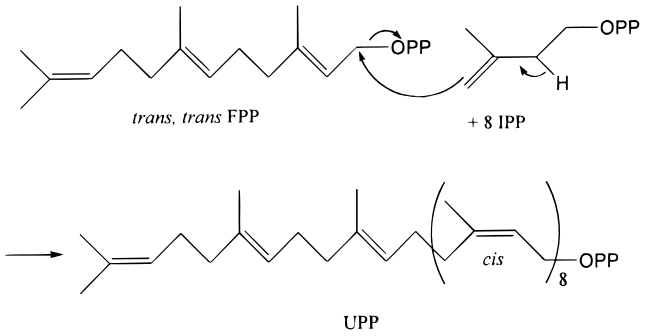

[a] The *trans,trans*-FPP couples with eight molecules of IPP to form undecaprenyl pyrophosphate. The newly formed double bonds are all in cis configuration.

† This work was supported in part by a grant from Academia Sinica.

* To whom correspondence should be addressed. Phone: 886-2-2785-5696 ext. 6070. Fax: 886-2-2788-9759. E-mail: phliang@gate.sinica.edu.tw.

[1] Abbreviations: UPPs, undecaprenyl pyrophosphate synthase; UPP, undecaprenyl pyrophosphate; IPP, isopentenyl pyrophosphate; FPP, farnesyl pyrophosphate; SPPs, solanesyl pyrophosphate synthase; PP_i, pyrophosphate; polymerase chain reaction, PCR; IPTG, isopropyl-*β*-D-thiogalactopyranoside; NiNTA, nickel nitrilo-tri-acetic acid; Tris, tris-(hydroxymethyl)aminomethane; Hepes, 4-(2-hydroxyethyl)-1-piperazineethanesulfonic acid; EDTA, ethylenediaminetetraacetic acid; SDS−PAGE, sodium dodecyl sulfate-polyacrylamide; dNTP, deoxynucleoside 5′-triphosphate

10.1021/bi000992l CCC: $19.00
Published on Web 08/12/2000

product formation or dissociation is the rate-determining step. Furthermore, in the UPPs reaction, there are eight IPP condensation reactions and each (except the first reaction) involves pyrophosphate (PP_i) dissociation, relocation of newly formed allylic pyrophosphate, IPP binding, and chemical bond cleavage and formation. It is still not known which of the steps is rate limiting in the presence and absence of Triton for UPPs reaction. The steady-state kinetic measurements performed previously provided only limited information in the reaction mechanism (*11*, *14*, *15*).

The aim of this study is to examine the multiple-step UPPs kinetics and define reaction mechanism using pre-steady-state kinetic approaches. First, a large quantity of UPPs was prepared by expressing the protein in *Escherichia coli* with N-terminal His-tag to facilitate its purification using NiNTA column chromatography and tag cleavage by FXa protease. The UPPs reactions using FPP and IPP as substrates were preformed under various conditions including a condition of [E] > [IPP] to examine the product distribution. Reaction kinetics under single-turnover, multiple-turnover and steady-state conditions in the presence and absence of Triton were also measured to identify the rate-limiting step.

EXPERIMENTAL PROCEDURES

Chemicals. [^{14}C]IPP (55 mCi/mmol) radiolabeled substrate was purchased from Amersham Pharmacia Biotech. The FPP was product of Sigma Co. Reversed-phase TLC for product analysis was obtained from Merck chemical Co. Taq DNA polymerase was purchased from Gibco. The plasmid miniprep kit, DNA gel extraction kit, and NiNTA resin were the products of QIAGEN. Potato acidic phosphatase (2 units/mg) was purchased from Boehringer Mannheimer. FXa cleavage kit containing FXa and Xarrest Agarose (for protease capture) was obtained from Novagen. Millipore ultrapure water was exclusively used in our studies. All buffer and other reagents were of the highest commercial purity.

Overproduction of UPPs from E. coli Bos-12 with N-Terminal His-Tag. The primers for amplification of gene encoding UPPs from *E. coli* Bos-12 genome DNAs using polymerase chain reaction (PCR) are shown as following with 5′ ATGTTGTCTGCTACTCAACCACTTAG 3′ as forward primer and 5′ ATCAGGCTGTTTCATCACCG 3′ as reverse primer. The amplified UPPs gene was purified from 0.8% agarose gel electrophoresis and used as a PCR template. The second PCR was performed using the primers with the FXa cleavage site (IEGR) and the complementary sequences of the sticky ends of the vector pET-32Xa/LIC (Novagen). The forward primer was 5′ GGTATTGAGGGTCGCATGTTGTCTGCT 3′ and reverse primer was 5′ AGAGGAGAGTTAGAGCCATCAGGCTGT 3′. The PCR gene product was purified and digested with T4 polymerase to create sticky 3′ and 5′ ends for ligation into LIC site of the vector. The recombinant plasmid was then transformed into NovaBlue cell (Novagen) for selection of the colonies containing engineered plasmid and the UPPs gene was sequenced. Finally, the plasmid with correct UPPs gene sequence was transformed into expression host *E. coli* BL21 (DE-3) (Novagen). Single transformant was grown up overnight at 37 °C in LB containing ampicillin (100 μg/mL). The 5 mL overnight cultures were used to inoculate 2 L of fresh LB medium containing 100 μg/mL ampicillin and allowed to grow to OD_{600} 0.6 before induction with 1 mM IPTG (final concentration). The cultures were induced for 3−4 h and harvested by centrifuge. Cell pellets were frozen and stored at −70 °C prior to purification.

Purification of His-Tagged UPPs and Removal of Tag. Enzyme purification was carried out at 4 °C. The 2 L cell culture was collected to yield approximately 20 g of Cell paste. The cell paste was suspended in 80 mL of lysis buffer containing 25 mM Tris (pH 7.5), and 150 mM NaCl. French-press apparatus (AIM-AMINCO spectronic Instruments) was used to break the cells at 12,000 psi. The lysis solution was centrifuged and the debris was discarded. The cell free extract was loaded into a 20 mL of NiNTA column which was equilibrated with 25 mM Tris (pH 7.5) containing 150 mM NaCl and 5 mM imidazole. The column was washed with 5 mM imidazole followed by 30 mM imidazole-containing buffer. The His-tagged UPPs was eluted with 25 mM Tris (pH 7.5), 150 mM NaCl, and 300 mM imidazole. The protein solution was dialyzed against 2 × 2 L buffer (25 mM Tris, pH 7.5, and 150 mM NaCl).

The His-tagged UPPs was digested with FXa protease to remove the tag. The Xarrest Agarose was added to untagged UPPs mixture to capture the FXa and the agarose was removed by centrifuge. The solution was then loaded onto NiNTA. The UPPs in flow through (25 mM Tris, pH7.5, 150 mM NaCl, and 5 mM imidazole) was highly pure according to SDS−PAGE and was dialyzed to buffer (25 mM Tris, pH 7.5, and 150 mM NaCl) for storage. The purified protein was confirmed by N-terminal sequencing and mass spectrum. The enzyme concentration used in all experiments was determined from the absorbance at 280 nm.

Products Formation and Analysis. The reaction mixture containing UPPs, [^{14}C]IPP, FPP, 0.5 mM $MgCl_2$, and 50 mM KCl and with or without Triton in 100 mM Hepes buffer (pH 7.5) was incubated at 25 °C to allow the reaction go to completion and the reaction was terminated with 10 mM EDTA. The reaction time in the presence of 0.1% Triton and absence of Triton was 0.5 and 5 h, respectively. Radiolabeled polyprenyl pyrophosphates formed were extracted with 1-butanol (IPP was in aqueous phase). After the removal of 1-butanol by evaporation, the 20% propanol solution containing 4.4 U/mL acidic phosphatase, 0.1% Triton, and 50 mM sodium acetate (pH 4.7) was used to convert polyprenyl pyrophosphate products to the corresponding alcohols (*16*). Upon the completion of the pyrophosphate hydrolysis catalyzed by the acidic phosphatase, the polyprenols were extracted with *n*-hexane. The hexane volume was reduced by evaporation and the residual solution was spotted on reverse phase TLC. The TLC plate was developed using acetone/water (19:1) as mobile phase (*5*). The plate with radiolabeled products was exposed to a film and the radioactivity distribution was determined by autoradiography with a bioimaging analyzer (FUJIFILM BAS-1500). The products were identified by the R_f values as previously reported (*5*).

Steady-State K_m and k_{cat} Measurements.[2] The enzyme reaction was initiated by adding 0.01 μM UPPs to a mixture containing various concentrations of FPP (0.1−5 μM) and [^{14}C]IPP (1−50 μM) in 100 mM Hepes buffer (pH 7.5), 50

[2] The k_{cat} is defined for IPP monomer incorporation and not for complete cycle for UPP formation.

M KCl, and 0.5 mM $MgCl_2$, at 25 °C in the presence or absence of 0.1% Triton X-100. Within 10% substrate depletion, the reaction mixture was periodically withdrawn. The reaction was terminated by adding 10 mM EDTA and the product was extracted with 1-butanol. The initial rate was calculated by plotting the [IPP] consumed versus time within 10% product formation.

Rapid Chemical Quench Experiments. The rapid-quench experiments were performed using a Kintek RFQ-3 Rapid Chemical Quench apparatus (Kintek Instruments, Texas). For the single-turnover experiments, the reaction was performed under the condition of [E] > [FPP] and sufficient [^{14}C]IPP was used to complete one cycle of UPP formation. The reaction was initiated by mixing 15 μL of the enzyme (10 μM) preincubated with FPP (1.07 μM) with equal volume of [^{14}C]IPP (50 μM) solution in buffer containing 100 mM Hepes (pH 7.5), 0.5 mM $MgCl_2$, 50 mM KCl, at 25 °C and with or without 0.1% Triton. In all cases, the concentrations of enzyme and substrates cited in the text are those after mixing and during the enzymatic reaction. The enzyme reaction was terminated by quenching with 67 μL of 0.6 N NaOH to give a final concentration of 0.46 N NaOH. A control was included with each experiment to ensure that the base was terminating the enzyme catalysis. This involved adding the substrates to a premixed solution of base and enzyme. The 0.46 N NaOH was found to be satisfactory as quenching agent. We have tried using 100 mM EDTA or 0.6 N HCl as quenching agent, but both failed to immediately stop the reaction (the reaction still proceeded after quenching for sub-sec). The polyprenyl pyrophosphates were stable under basic condition and can be extracted with 1-butanol. The reaction mixture quenched with 0.46 N NaOH was extracted with the same volume of butanol twice and the radioactivity in the organic phase (intermediates and product) was counted using a Beckmann LS6500 scintillation counter. The single-turnover time course was composed of the radiolabeled IPP consumption (the sum of the IPP incorporated into intermediates and product) in a specified reaction time. For intermediates and product identification at each time point, we have utilized 1-butanol to extract the reaction mixture, evaporated solvent under N_2, prepared the 20% propanol solution containing acidic pyrophosphatase and analyzed the polyprenols formed by TLC as described above. We have thus obtained the time course for each intermediate, which is related to its rates of formation and decomposition. The data for each intermediate time course and the single-turnover reaction were simulated by a kinetic simulation computer program KINSIM as described below.

A multiple-turnover experiment using 0.75 μM enzyme, 50 μM [^{14}C]IPP, and 6 μM FPP was also performed. The enzyme preincubated with FPP was mixed with radiolabeled IPP at 25 °C in the buffer containing 100 mM Hepes (pH 7.5), 0.5 mM $MgCl_2$, and 50 mM KCl in the absence of Triton. The reaction was terminated by 0.6 N NaOH and the products were extracted with butanol. The product formation was quantitated from the radioactivity level in the butanol phase. The products were analyzed using the same procedure described above and the KINSIM program was used to simulate the time course of the reaction.

Data Simulation. The KINSIM kinetic simulation program (*17*) was used to model all of the kinetic data presented in this paper based on the reaction pathway shown in Scheme 2. The program allows the input of data as *x*,*y* pairs from rapid-quench experiments. The data were fit by a trial and error process to minimize the sum square errors in fitting the data. The K_m and k_{cat} values were used to constrain the fitting. The irreversity of the IPP condensation reaction has simplified the simulation process since only one rate constant was needed for each IPP condensation step. The enzyme reaction model and estimated rate constants described in Scheme 2 were calculated from KINSIM fitting of our kinetic data. In this model, UPPs binds FPP and IPP and then catalyzes eight continuous IPP condensation steps leading to the final product C_{55}−UPP with eight rate constants which were deduced from the time courses of intermediates in the single-turnover reaction with Triton. For the single-turnover and multiple-turnover reactions in the absence of Triton, the formation of extra products C_{60}, C_{65}, C_{70}, and C_{75} polyprenyl pyrophosphates were also included in the simulation. The rapid-quench reactions were conducted under the condition that [E] ≫ K_m for FPP (and likely for intermediates) so the dissociation of E·intermediate was not included in Scheme 2. The details of the kinetic simulation of the data in this study are attached as the Supporting Information. Although at this stage, the association and dissociation constants for the reaction species are unknown, the experiments were performed under the condition where binding was not rate limiting or the substrate was preincubated with enzyme. These binding rate constants used in our kinetic model therefore do not change the interpretation of the reaction mechanism.

Scheme 2: Proposed Kinetic Pathway for UPPs Catalyzed Reaction

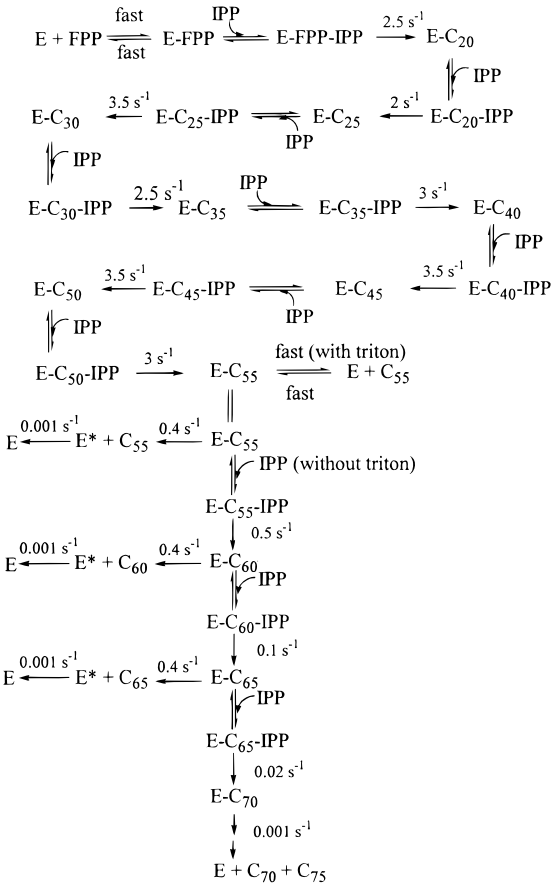

Table 1: Quantification of Product Distribution of UPPs Catalyzed Coupling of FPP and IPP under Various Reaction Conditions

condition	C_{20}	C_{25}	C_{30}	C_{35}	C_{40}	C_{45}	C_{50}	C_{55}	C_{60}	C_{65}	C_{70}
0.2 μM E, 50 μM FPP, 50 μM IPP, 0.1% Triton			11.18	4.16	3.71	13.87	34.08	34.39			
0.2 μM E, 5 μM FPP, 50 μM IPP, 0.1% Triton								100			
10 μM E, 50 μM FPP, 1 μM IPP, 0.1% Triton	29.24	20.34	13.04	8.59	4.97	5.83	9.09	8.91			
10 μM E, 0.1 μM FPP, 1 μM IPP, 0.1% Triton								100			
0.2 μM E, 50 μM FPP, 50 μM IPP		3.68	7.56	7.74	4.63	20.93	18.75	16.36	9.01	6.76	
0.2 μM E, 5 μM FPP, 50 μM IPP							11.60	50.31	12.98	11.17	13.94
10 μM E, 50 μM FPP, 1 μM IPP	47.33	32.60	10.83	4.13	1.67	1.29	1.32	0.83			
10 μM E, 0.1 μM FPP, 1 μM IPP								57.38	42.62		

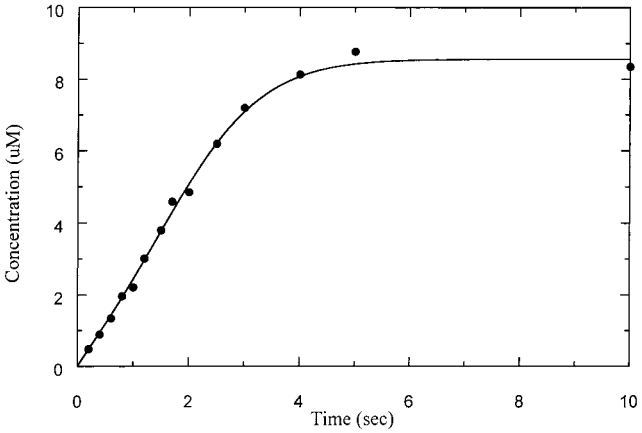

FIGURE 1: The single-turnover rapid-quench experiment of UPPs reaction with enzyme in excess of FPP. A solution containing enzyme (10 μM) preincubated with FPP (1.07 μM) was mixed with [^{14}C]IPP (50 μM) at pH 7.5 and 25 °C in the presence of 0.1% Triton. The curve represents a fit by KINSIM simulation using rate constants shown in Scheme 2.

RESULTS

Product Distribution of UPPs Reaction under Various Conditions. The UPPs reactions were performed under a variety of conditions and the final products formed were examined. The results of these studies are summarized in Table 1 and the imaging data are shown in Figure 1 of the Supporting Information. Although it was previously reported that C_{55}−UPP was the primary product (*4*), we found a significant amount of intermediates under some reaction conditions using *E. coli* UPPs. As shown in row 1 of Table 1, under multiple turnovers with 0.2 μM enzyme, 50 μM [^{14}C]IPP, and 50 μM FPP in the presence of Triton, the C_{25}−C_{50} intermediates were formed, in addition to UPP. However, with the decrease of FPP concentration to 5 μM ([FPP]:[IPP] = 1:10) as shown in row 2, UPP was the only product. By comparing the results of row 1 to row 2, it appears that high concentration of FPP could displace C_{25}−C_{50}-polyprenyl pyrophosphates from the enzyme active site. As demonstrated in row 5 and 6, under the same experimental condition corresponding to row 1 and 2, respectively, except that Triton was omitted, C_{60}−C_{75}-polyprenyl pyrophosphates were also produced and the intermediates accumulated under high concentration of FPP. These results are consistent with the slow release of the UPP in the absence of Triton, which led to the higher polymer formation.

The reaction shown in row 3 of Table 1 contained 10 μM UPPs and only 1 μM [^{14}C]IPP and excess of FPP (50 μM). Under such condition, the E·FPP complex concentration was 10-fold higher than IPP concentration and we expected that only C_{20}-geanylgeranyl pyrophosphate could form. However, the C_{20}, C_{25}, and C_{30} polymers were major products and the C_{35}−C_{50} intermediates plus UPP were still generated. As a control reaction shown in row 4, 10 μM enzyme catalyzed the single product UPP formation when FPP concentration was reduced to 0.1 μM and [^{14}C]IPP concentration remained the same ([FPP]:[IPP] = 1:10). The same reaction carried out in the absence of Triton also resulted in the formation of C_{20}, C_{25}, and C_{30} as major products (row 7) with the same concentration of FPP and [^{14}C]IPP. The C_{55} and C_{60} were the products formed under the condition of [FPP]: [IPP] = 1:10 as shown in row 8. The extra C_{60} formed in 10 μM enzyme with 0.1 μM FPP and 1 μM [^{14}C]IPP demonstrates that enzyme could accommodate larger polymer in the absence of Triton.

Steady-State K_m and k_{cat} Measurements. The K_m of IPP and FPP were 4.1 ± 0.3 and 0.4 ± 0.1 μM, respectively, and the k_{cat} value was 2.5 ± 0.1 s^{-1} measured from the varied concentrations of [^{14}C]IPP and FPP. In contrast, 0.01 μM of UPPs with 5 μM of FPP and 50 μM of [^{14}C]IPP, 0.5 mM $MgCl_2$, and 50 mM KCl in Hepes buffer (pH 7.5) was 190-fold less active (0.013 ± 0.001 s^{-1}) for the IPP consumption in the absence of Triton. This was consistent with the finding that Triton and phospholipid activated UPPs activity (*4*). To understand the Triton effect, we attempted to perform single-turnover experiments where enzyme was in excess and product release needs not be considered. The rate measured with or without Triton should be the same provided that Triton only enhances the product release rate but does not alter the chemical rate.

Single-Turnover Reaction Kinetics. The substrate consumption was examined under single-turnover ([E] > [FPP]) condition with 1.07 μM FPP and 10 μM enzyme saturated with 50 μM [^{14}C]IPP in the presence of 0.1% Triton. In this single-turnover experiment, the intermediates and product can be clearly seen as shown in Figure 2A (Supporting Information) and the concentration of each intermediate and product at each time point can be determined. The KINSIM program was used to fit each intermediate time course (see Figure 2) to obtain the rate constant of individual IPP condensation. The kinetic pathway of UPPs reaction with assigned rate constant is summarized in Scheme 2. The fit of Figure 1 was thus obtained from the sum of radiolabeled [IPP] included in each intermediate and product at each time point simulated by KINSIM program. The rate constants of IPP condensations in Scheme 2 were similar to k_{cat} value suggesting that the IPP coupling rather than product release is rate limiting in the presence of Triton. There was no change in the rate of catalysis under conditions in which IPP concentration was doubled or IPP was preincubated with enzyme, indicating that IPP binding was not rate limiting under experimental conditions (data not shown). In the

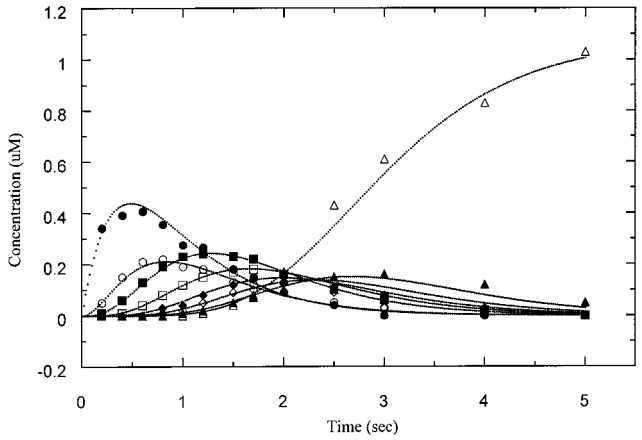

FIGURE 2: UPPs catalyzed time courses of intermediates (C_{20}−C_{50}) and product (C_{55}). The reaction was performed under single-turnover condition where UPPs (10 μM) preincubated with FPP (1.07 μM) was mixed with [^{14}C]IPP (50 μM) at pH 7.5 and 25 °C in the presence of 0.1% Triton. The data represent the time courses of C_{20} (●), C_{25} (○), C_{30} (■), C_{35} (□), C_{40} (◆), C_{45} (◇), C_{50} (▲), and C_{55} (△). The fitting curves were generated from KINSIM program.

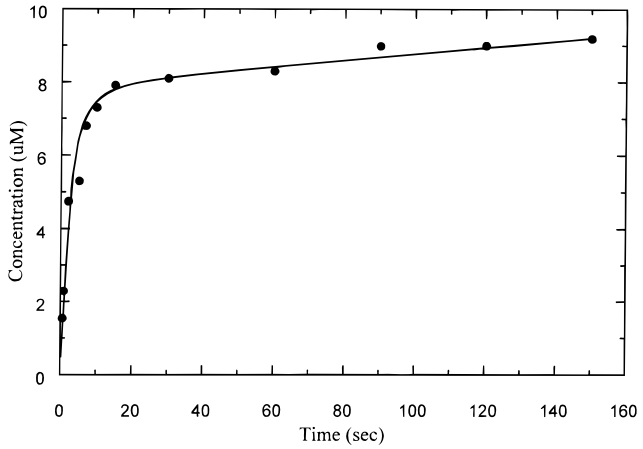

FIGURE 3: A pre-steady-state burst of product for UPPs reaction in the absence of Triton. A solution containing enzyme (0.75 μM) preincubated with FPP (6 μM) was mixed with [^{14}C]IPP (50 μM) at pH 7.5 and 25 °C. The curve was obtained using the rate constants shown in Scheme 2 by KINSIM simulation.

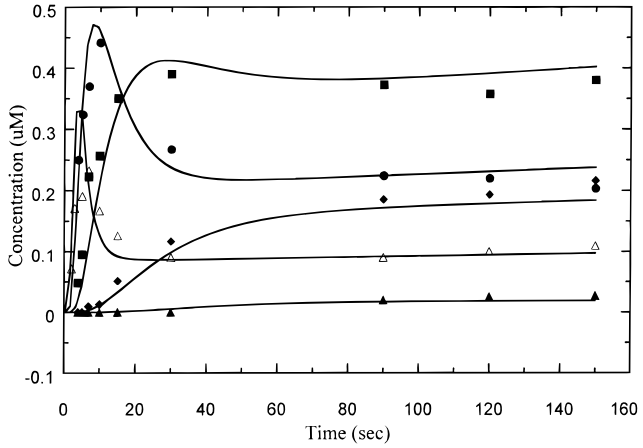

FIGURE 4: The time courses of C_{55}, C_{60}, C_{65}, C_{70}, and C_{75} in the multiple enzyme turnovers in the absence of Triton with 0.75 μM UPPs, 6 μM FPP, and 50 μM [^{14}C]IPP at pH 7.5 and 25 °C. The data indicate formation of C_{55} (△), C_{60} (●), C_{65} (■), C_{70} (◆), and C_{75} (▲) polyprenyl pyrophosphates. The solid lines represent the fits from KINSIM simulation using the rate constants in Scheme 2.

absence of Triton, similar time course of single-turnover reaction and similar intermediate accumulation level were obtained except that C_{55} and higher polymers became the final products (Figure 2B, Supporting Information). It is possible that the active site of the enzyme assumed a different protein conformation in the absence of Triton to allow the generation of higher polymers in the presence of excess IPP. However, according to our data simulation, the $C_{55} \rightarrow C_{60}$, $C_{60} \rightarrow C_{65}$, and $C_{65} \rightarrow C_{70}$ steps in the absence of Triton had approximately 5-fold (0.5 s^{-1}), 25-fold (0.1 s^{-1}), and 125-fold (0.02 s^{-1}) lower rate than k_{cat}. Therefore, without Triton, the UPPs steady-state rate is 190-fold slower but the single-turnover rate for the formation of UPP remained unchanged. These experiments have demonstrated that Triton can activate UPPs activity by accelerating a step after IPP condensation reactions.

Pre-Steady-State Burst of Product Formation. Since a post-chemistry step is much slower than the conversion of substrates to products in the absence of Triton, we examined enzyme multiple turnovers with 0.75 μM enzyme mixed with 50 μM [^{14}C]IPP and 6 μM FPP. The burst product formation was observed as shown in Figure 3. The C_{55}, C_{60}, C_{65}, C_{70}, and small amount of C_{75} polymers were found as the final products in the absence of Triton as shown in Figure 3 of Supporting Information. Therefore, these steps had to be included in the simulation process. The rate constant of the rate-limiting step in the absence of Triton can be estimated from the steady-state rate divided by the average number of IPP incorporated into the final products. This rate constant 0.001 s^{-1} was used in the KINSIM simulation as the rate of a slow product dissociation or other step. If the C_{55}, C_{60}, and C_{65} dissociated from the enzyme at a rate of only 0.001 s^{-1} during the progressive polymerization, each of these intermediates should have returned to the baseline. Instead, the C_{55}, C_{60}, and C_{65} accumulated, which indicated that a significant fraction of the C_{55}, C_{60}, and C_{65} dissociated at each round of polymerization. To fit the time courses of the C_{55}, C_{60}, and C_{65} formations in the linear phase of the multiple enzyme turnovers, the C_{55}, C_{60}, and C_{65} dissociation rates were approximately 0.4 s^{-1} in order to account for their accumulation levels. The KINSIM simulation on the C_{55}−C_{75} time courses is shown in Figure 4. A slow step after polyprenyl pyrophosphate product dissociation for enzyme to undergo the next turnover needs to be included in the reaction mechanism (see Scheme 2) to account for the steady-state rate in the absence of Triton. Since the $C_{70} \rightarrow C_{75}$ reaction is extremely slow (approaching 0.001 s^{-1}), C_{70} can dissociate from the active site at 0.4 or 0.001 s^{-1} without affecting the accumulation levels of C_{55}, C_{60}, and C_{65}. The details of the KINSIM simulation are summarized in Charts 1 and 2 of the Supporting Information for enzyme single turnover and multiple turnovers, respectively. The rate-limiting step is unlikely to be associated with pyrophosphate release since the PP_i release was not that slow judging from the IPP condensation. This rate-limiting step likely represents a protein conformational change to adopt the much smaller FPP for the next enzyme turnover. The data in Figure 3 can then fit by a scheme using a set of rate constants including chemical step rates as described above, the slow product

dissociation rates and an even slower enzyme conformational change rate in the absence of Triton (see Scheme 2). Therefore, the rate-determining step for UPPs reaction under steady-state condition in the absence of Triton might be an enzyme conformational change after product dissociation.

DISCUSSION

C_{55}−UPP has been identified as a lipid carrier to transport the intracellular carbohydrates to outside of the cell membrane for cell wall glycoconjugates assemblies. Apparently, the major function of UPPs is mediating the synthesis of UPP. The C_{55}-polyprenyl pyrophosphate was previously identified as the primary product synthesized from FPP and IPP for UPPs. We have utilized various conditions to examine the product of *E. coli* UPPs reaction and found significant accumulation of intermediates when FPP was in excess. In vitro, FPP appears to be capable of displacing intermediates under the condition of 50 μM of FPP and equal concentration of IPP. This is consistent with the high affinity of FPP (low K_m value) for *E. coli* UPPs. Therefore, for efficient in-vivo biosynthesis of UPP, the intracellular FPP and IPP concentrations should be accurately controlled to avoid the waste of these substrates. In addition, under the condition with enzyme in 10-fold excess of IPP, C_{20}-, C_{25}-, and C_{30}-polyprenyl pyrophosphates were the major products in the presence and absence of Triton. The results suggested that IPP molecules were not all bound to E·FPP and resulting in C_{20}-geranylgeranyl pyrophosphate as sole product under the condition of [E·FPP] > [IPP]. Rather, more than one IPP were incorporated into E·FPP to generate the C_{25}−C_{55}-polyprenyl pyrophosphates. It is likely that the enzyme has a low affinity to IPP (high K_m value) and a high affinity to FPP (small K_m value) for capturing FPP and the subsequently formed E·intermediates have a higher affinity to IPP for the formation of product with the desired chain length. This was not displayed in Charts 1 and 2 of the Supporting Information for the reason of simplifying the kinetic data simulation (the IPP K_m value of each intermediate was assumed the same). It is however supported by our recent stopped-flow experiments measuring the binding of IPP to the complex of E·geranylgerany pyrophosphate (Liang et al., unpublished results). This model could be also tested for other prenyltransferases.

The product distribution pattern of UPPs is different from that of solanesyl pyrophosphate synthase (SPPs) which catalyzes a long-chain all-trans C_{45} polyprenyl pyrophosphate formation (*18*). In SPPs reaction, adding various amounts of FPP (0.25−25 μM) to constant IPP (25 μM) gave no difference in product distribution (octaprenyl pyrophosphate and solanesyl pyropohosphate were the major products in all cases). However, in the UPPs reaction, the intermediates were formed with 50 μM FPP and 50 μM IPP, but UPP was the only product when 5 μM FPP and 50 μM IPP were employed. This result indicates that the UPPs (Z-type) might have higher affinity for FPP or less affinity for intermediates than SPPs (E-type) which begins to generate the intermediate products when FPP was in 5-fold excess of IPP. The FPP K_m was 0.75 μM for *M. luteus* SPPs and 0.13 μM reported for UPPs isolated from *L. plantarum* (*19, 20*).

The K_m of IPP and FPP were determined to be 4.1 and 0.4 μM, respectively, and the k_{cat} value of the reaction was 2.5 s^{-1} in the presence of Triton for *E. coli* UPPs. This FPP K_m value is consistent with the reported K_m value of 0.13 μM for the purified *L. plantarum* UPPs (*20*), and deviated significantly from 8 and 9.1 μM measured for *M. luteus* and *B. subtilis* enzymes, respectively (*14*, *15*). The IPP K_m was also comparable with 1.92 μM measured for *L. plantaru*m enzyme (*20*). The steady-state k_{cat} value was similar to the rate constants obtained under UPPs single-turnover experiments, indicating IPP condensation is rate limiting under steady-state condition in the presence of Triton. For IPP condensation, several steps including PP_i dissociation, relocation of the newly formed allylic pyrophosphate for the next IPP condensation, IPP binding, and bond cleavage and formation for 1−4 condensation have to occur. The release of highly charged PP_i from its binding site and the relocation of allylic pyrophosphate (especially for large polymer) are not trivial in reaction kinetics. It was hypothesized that a conformational change caused by the release of highly charged PP_i could provide a driving force to move the intermediate allylic pyrophosphate to the proper position for next IPP condensation (*8*). In our single-turnover experiments, compared to the following IPP condensation steps, the $C_{15} \rightarrow C_{20}$ reaction had a similar observed rate, in which the enzyme was preincubated with FPP so that PP_i dissociation and allylic pyrophosphate relocation were not involved in the reaction. It appears that the bond forming or breaking during each IPP condensation was rate limiting. It is thought that the allylic cation formation is rate-limiting step for the 1−4 condensation and the Mg^{2+} plays a role in acceleration of the cation formation (*21*).

In the absence of Triton, the steady-state rate is only 0.013 s^{-1} that is much lower than the enzyme single-turnover rate determined in the absence of Triton. This suggested that a step after product formation is the rate-limiting step in the absence of Triton under steady-state condition. The pre-steady-state burst of product formation further supported this conclusion. The rate of fast phase and the rate of linear phase corresponded to the single-turnover rate and steady-state rate, respectively, in the absence of Triton. Judging from the level of accumulation of C_{55}, C_{60}, and C_{65}, the product dissociation rates need to be 0.4 s^{-1} for these intermediate products. Also, a 0.001 s^{-1} conformational change step after C_{55}, C_{60}, and C_{65} dissociation governs the steady-state rate of UPPs reaction in the absence of Triton. The accumulation of intermediate products was also observed previously for the progressive polymerization of DNA nucleotides catalyzed by the HIV reverse transcriptase (*22*). In that case, a product burst was observed under enzyme multiple turnovers and a product dissociation step after dNTP incorporation was proposed as rate-determining step. However, according to computer simulation of the accumulation levels of intermediates, the DNA release rate from E·DNA·dNTP needed to be faster than the observed steady-state rate constant. Another product release step (DNA dissociation from E·DNA) was then assigned as the rate-determining step in the reaction to account for the steady-state rate.

From the kinetic data presented here, the Triton effect on the activation of UPPs activity is apparently on the enhancement of the rate of product dissociation and the rate of a protein conformational change. The single-turnover reaction rate was similar in the presence or absence of Triton. However, the steady-state rate is largely accelerated by the

presence of Triton. The higher polyprenyl pyrophosphates ($C_{60}-C_{75}$) were formed in the absence of Triton, indicating that the UPPs has different conformation and product release was slow under such condition.

In summary, our kinetic data including steady-state and pre-steady-state experiments defined a set of rate constants for this complicated UPPs reaction containing eight IPP condensation steps. In the reaction pathway shown in Scheme 2, the individual IPP addition has a rate constant close to the k_{cat} value. However, the association and dissociation rate constants of FPP and IPP to the enzyme are still lacking at this stage and we performed the pre-steady-state experiments under the condition that binding was not rate limiting. Nevertheless, this enzyme reaction model deduced from our pre-steady-state kinetic studies provides an unambiguous basis for the interpretation of the catalytic function of this enzyme. The transient kinetic technologies might also be useful in inhibitor studies of UPPs and characterization of other Z- and E-type long chain polyprenyl-synthesizing enzymes such as solanesyl pyrophosphate synthase that requires a polyprenyl carrier protein for product transfer to maintain its catalytic efficiency (*19*).

ACKNOWLEDGMENT

We thank Dr. Teh-Yung Liu for helpful discussion and support.

SUPPORTING INFORMATION AVAILABLE

Imaging data (3 figures) and kinetic simulation (2 charts). This material is available free of charge via the Internet at http://pubs.acs.org.

REFERENCES

1. Robyt, J. (1998) in *Essentials of carbohydrate chemistry*, Chapter 10, pp 305−318, Springer-Verlag, New York.
2. Sutherland, I. W. (1977) in *Surface Carbohydrates of the Prokarotic Cell*, p 27, Academic Press, London.
3. Hussey, H., and Baddiley, (1976) *The Enzyms in Biological Membranes*, Vol. 2, p 227, Plenum, New York.
4. Allen, C. M. (1985) *Methods Enzymol. 110*, 281−299.
5. Shimizu, N., Koyama, T., and Ogura, K. (1998) *J. Biol. Chem. 273*, 19476−19481.
6. Apfel, C. M., Takacs, B., Fountoulakis, M., Stieger, M., and Keck, W. (1999) *J. Bacteriol. 181*, 483−492.
7. Ogura, K., and Koyama, T. (1998) *Chem. Rev. 98*, 1263−1276.
8. Ogura, K., Koyama, T., and Sagami, H. (1997) *Subcellular Biochem. 28*, Chapter 3, 57−87.
9. Baba, T., and Allen, C. M. (1980) *Arch. Biochem. Biophys. 200*, 474−484.
10. Allen, C. M., Keenan, M. V., and Sack, J. (1976) *Arch. Biochem. Biophys. 175*, 236−248.
11. Keenan M. V., and Allen, C. M. (1974) *Arch. Biochem. Biophys. 161*, 375−383.
12. Allen, C. M., and Muth, J. D. (1977) *Biochemistry 16*, 2908−2915.
13. Keenan, M. V., and Allen, C. M. (1974) *Biochem. Biophys. Res. Commun. 61*, 338−342.
14. Baba, T., and Allen, C. M. (1978) *Biochemistry 17*, 5598−5604.
15. Takahashi, I., and Ogura, K. (1982) *J. Biochem. (Tokyo) 92*, 1527-
16. Fujii, H., Koyama, T., and Ogura, K. (1982) *Biochim. Biophys. Acta 712*, 716−718.
17. Barshop, B. A., Wrenn, R. F., and Frieden, C. (1983) *Anal. Biochem. 130*, 134−145.
18. Ohnuma, S.-I., Koyama, T., and Ogura, K. (1992) *J. Biochem. (Tokyo) 112*, 743−749.
19. Ohnuma, S.-I., Koyama, T., and Ogura, K. (1991) *J. Biol. Chem. 266*, 23706−23713.
20. Muth, J. D., and Allen, C. M. (1984) *Arch. Biochem. Biophys. 230*, 49−60.
21. Poulter, C. D., and Rilling, H. C. (1982) in *Biosynthesis of Isoprenoid Compounds* (Porter, J. W., and Spurgeon, S. L., Eds.) Vol. 1, pp 161−224, John Wiley & Sons, New York.
22. Kati, W. M., Johnson, K. A., Jerva, L. F., and Anderson, K. S. (1992) *J. Biol. Chem. 267*, 25988−25997.

BI000992L